Supporting Information

A molten calcium carbonate mediator for the electrochemical conversion and absorption of carbon dioxide

Xiang Chen[1], Haijia Zhao[1], Jiakang Qu[1], Diyong Tang[2], Zhuqing Zhao[1], Hongwei Xie[1], Dihua Wang[2], Huayi Yin*[1,3]

1. Key Laboratory for Ecological Metallurgy of Multimetallic Mineral of Ministry of Education, School of Metallurgy, Northeastern University, Shenyang, P. R. China, 110819

2. School of Resource and Environmental Science, Wuhan University, Wuhan, P.R. China, 430072

3. Key Laboratory of Data Analytics and Optimization for Smart Industry, Ministry of Education, Northeastern University, Shenyang, P. R. China,110819

Email: yinhy@smm.neu.edu.cn

Experimental

Sodium-storage performance of electrolytic carbons

The sodium-storage performance of the electrolytic carbon was evaluated in half-type coin cells (CR2032). First, a slurry was made by mixing electrolytic carbon, Super P, and sodium carboxymethylcellulose (CMC) (8: 1: 1, weight ratio) were mixed with deionized water. Then, the slurry was coated on copper foil, which was vacuum-dried at 80 ^{o}C for 12 h and cut into discs that were used as the working electrode. A glass fiber film (Whatman GF/D) and a sodium foil served as the separator and the counter electrode, respectively, and 1 M $NaClO_4$ dissolved in the mixture solution of propylene carbonate with 5% fluoroethylene carbonate (FEC) was the electrolyte. Galvanostatic charge-discharge measurements were carried out by a Land CT2001A battery system at a potential window of 0.005 - 3.0 V (*vs.* Na^+/Na). CV measurements were performed at a scan rate of 0.1 mV s^{-1}, and electrochemical impedance spectroscopy (EIS) was conducted at open circuit potential with a voltage amplitude of 5 mV and in a frequency range of 100 kHz to 10 mHz on an electrochemical workstation (Metrohm Autolab PGSTA302N, Eco Chemie B. V., Co. Ltd., Netherlands).

Characterization of porous carbon

The electrolytic carbon (710 ^{o}C at 3.0 V) are mesoporous carbon exhibiting a typical IV-type isotherm with a type H3 hysteresis loop (**Fig. S6**)[1]. In addition, the high adsorbed volume at low-down relative pressures is a typical result for microporous[2]. This evolution of mesoporous and microporous contributes extra specific surface area with a BET surface area of 435.6 m^2 g^{-1} and the specific surface area decreases with increasing the temperature (**Table**

S2). The pore sizes of carbon sample obtained under 710 °C range from both 3 to 4 dominantly. When the temperature is above 710 °C, the carbon materials show a combined typical II/IV-typle isotherms (**Fig. S6a**), and the pores with a diameter ranges from 31 to 92 nm (**Fig. S6b**). All carbon samples obtained at 710 °C exhibit a type IV characteristic with an obvious capillary condensation, indicating that the electrolytic carbons have mesoporous nature (**Fig. S6c**), and the pore size distribution curves reach at 3.8 nm (the inset of **Fig. S6d**).

Tab. S1. Summary of electrochemical reduction of CO_2 in high-temperature molten salts [3-20].

Electrolyte components	Temperature	Atmosphere	Anode	Reference
Li_2CO_3 Li_2CO_3-Na_2CO_3-K_2CO_3	750°C	Ar/CO_2	Gold-20% Palladinm crucible	Ingram et al. (1966)[3]
LiCl-KCl-K_2CO_3	450°C	----	Glass carbon	Kawamura et al. (2000)[4]
LiCl-Li_2CO_3 LiCl-NaCl-Na_2CO_3 LiCl-$CaCl_2$-CaO	700°C 650°C~800°C 600°C	CO_2	Graphite/Pt	Jianbang Ge et al. (2015~2017)[5-7]
LiCl-KCl-$CaCO_3$ Li_2CO_3-LiCl-KCl	450°C~650°C 450°C	CO_2	Graphite	Bowen Deng (2017~2018)[8]
$CaCl_2$-$CaCO_3$-LiCl-KCl Li_2CO_3-K_2CO_3	500°C~800°C	Ar/CO_2 N_2-CO_2	SnO_2	Happiness V. Ijije et al. (2014)[9, 10]
Li_2CO_3-Na_2CO_3-K_2CO_3	500°C	CO_2	SnO_2	Huayi Yin et al. (2013)[11]
Li_2CO_3	750°C~900°C	CO_2	Pt	Stuart Licht et al. (2010)[12]
LiF-Li_2CO_3 LiF-NaF-Li_2CO_3	700°C	CO_2	Pt/Graphite	Liangxing Li et al. (2014~2016)[13, 14]
Li_2CO_3-Na_2CO_3-K_2CO_3	450°C~700°C	CO_2	Graphite	K. Le Van et al. (2009)[15]
Li_2CO_3-Na_2CO_3-K_2CO_3	450°C~650°C	CO_2	SnO_2	Diyong Tang (2013)[16]

Li_2CO_3-Na_2CO_3-K_2CO_3	450°C	CO_2	Au	B.Kaplan (2002)[17]
Li_2CO_3-K_2CO_3 Li_2CO_3-Na_2CO_3	575°C~650°C	CO_2-Ar	Au	D.Chery (2014)[18]
LiCl-KCl-$CaCl_2$-CaC_2	550°C	----	Graphite	Chen et al. (2016)[19]
Li_2CO_3-K_2CO_3-Na_2CO_3	500°C~700°C	CO_2	Graphite	Hughes et al. (2018)[20]

Tab. S2. Summary of nitrogen adsorption-desorption tests for the electrolytic carbons.

Temperature (°C)	Cell voltage (V)	S_{BET} (m^2 g^{-1})	Discharge capacity (last cycle) SIBs (mAh g^{-1})
710	2.4	176.650	-
710	2.8	338.902	-
710	3.0	435.610	210
710	3.4	257.074	-
750	3.0	47.984	171.5
800	3.0	65.179	131.7
850	3.0	33.764	113.5

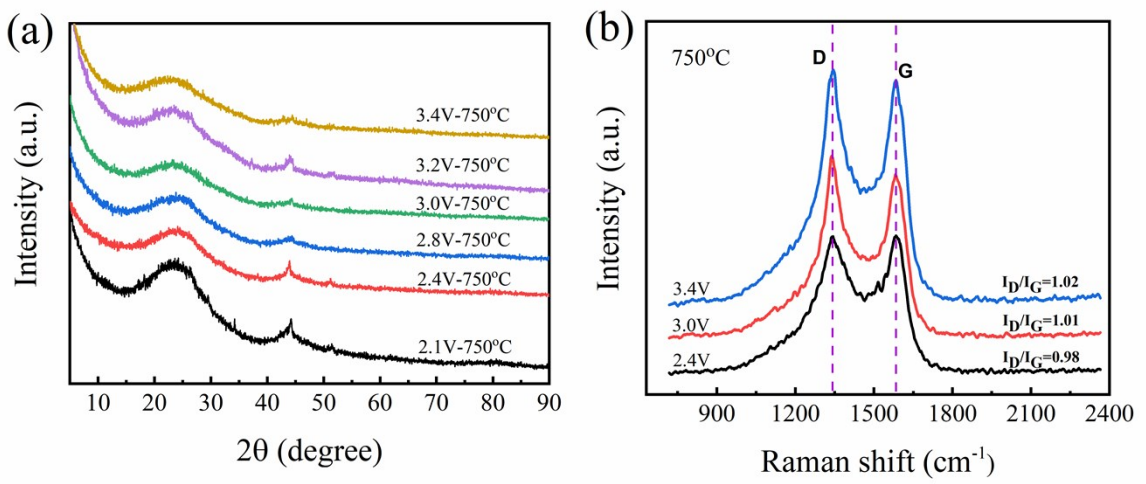

Fig. S1. (a) XRD patterns and (b) Raman spectra of the electrolytic carbons obtained at 750 °C and under cell voltages from 2.1 to 3.4 V.

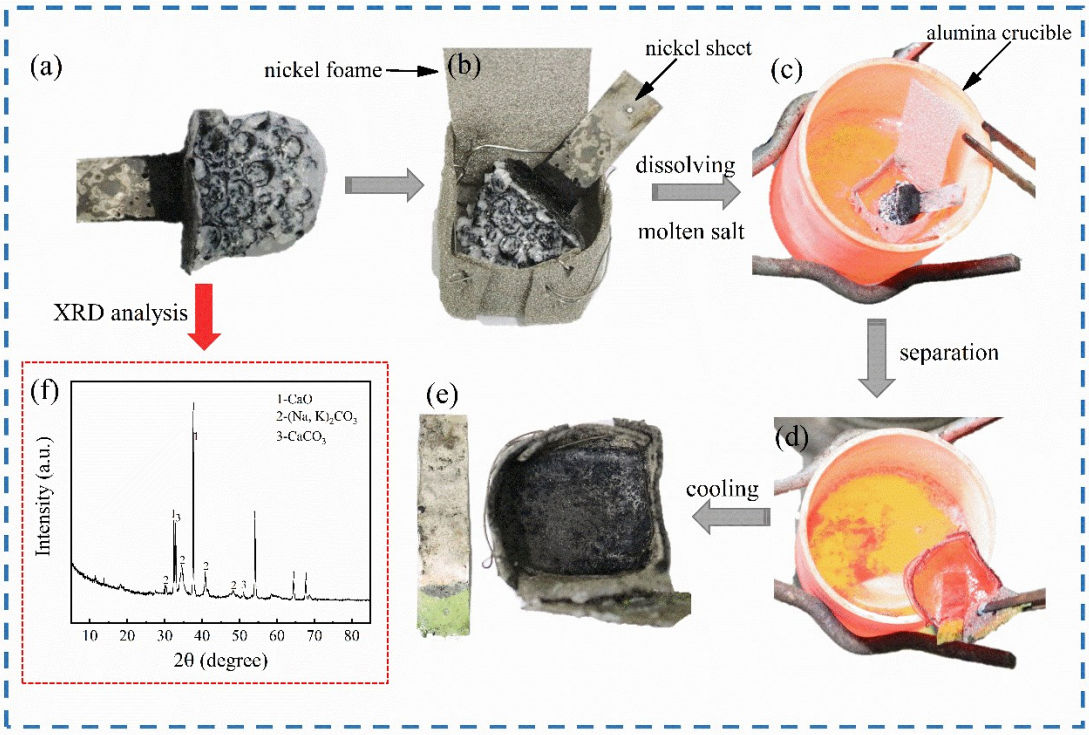

Fig. S2. Optical photographs of (a) electrolytic carbon, (b) electrolytic carbon wrapped in a nickel-foam foil, (c-d) an Al_2O_3 crucible filled with molten $CaCl_2$ for soaking the electrolytic product, (e) electrolytic product after soaking in $CaCl_2$, and (f) XRD pattern of the electrolytic product.

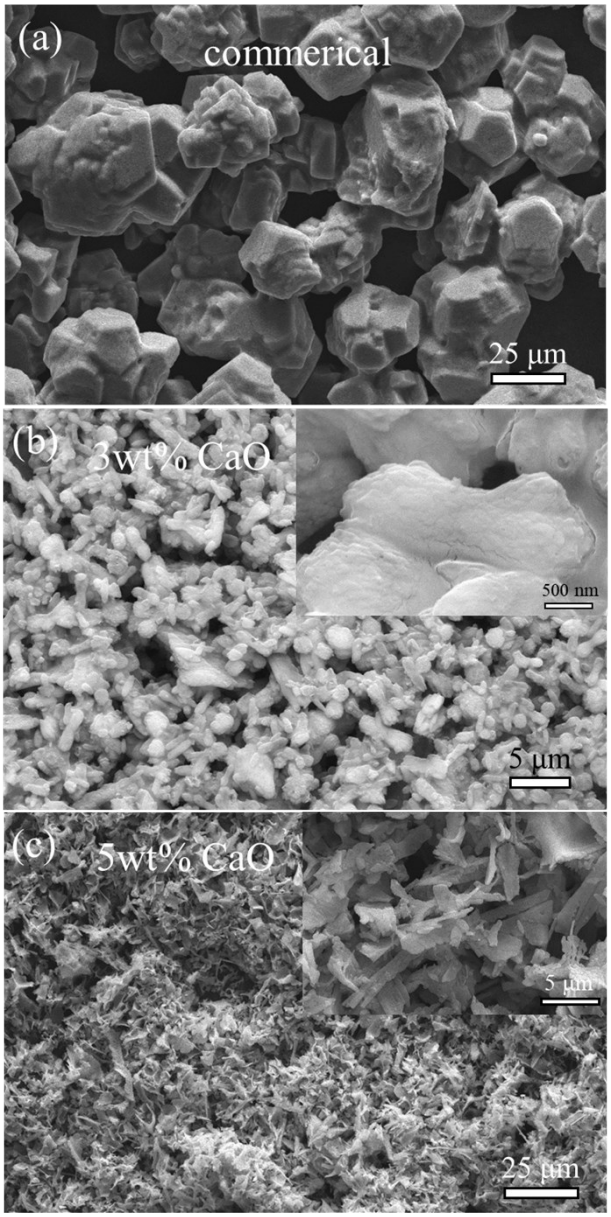

Fig. S3. The SEM images of (a) the commercial $CaCO_3$ and $CaCO_3$ derived CO_2 absorbing-convension in molten $CaCl_2$ with (b) 3 wt% and (c) 5 wt% CaO.

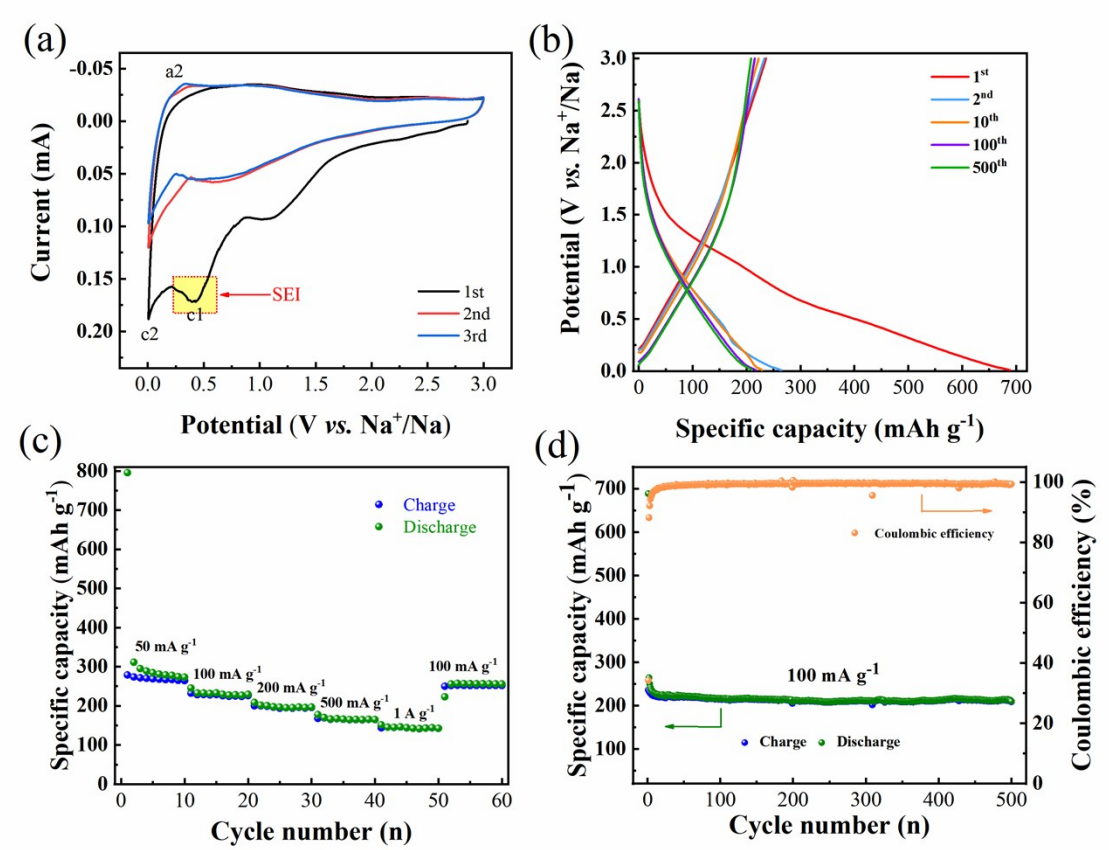

Fig. S4. Sodium-storage performances of the EC-710-3.0 electrode. (a) CV curves at 0.1 mV s^{-1}, (b) charge-discharge profiles at 1st, 2nd, 10th, 100th and 500th cycle, (c) rate performances, and (d) cycling performances at 100 mA g^{-1}.

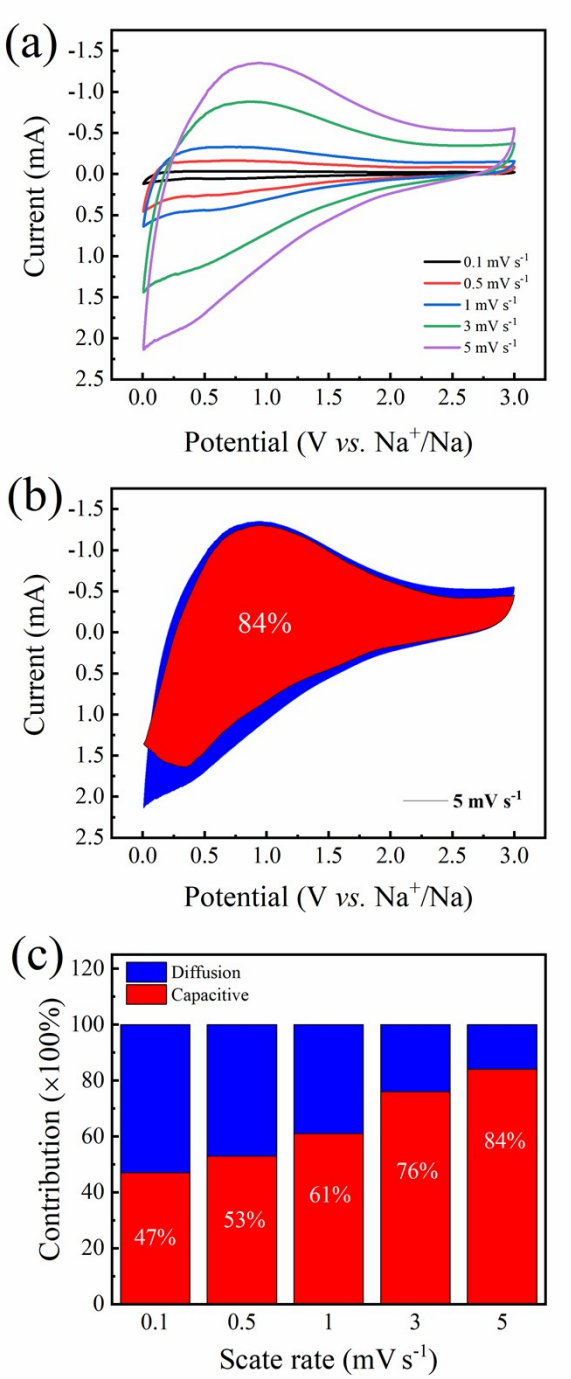

Fig. S5. (a) CVs of EC-3.0V-710 electrode at various scan rates. (b) Capacitive and diffusion contributions to the charge storage at 5mV s^{-1}. (c) Capacitive contribution ratios at different scan rates.

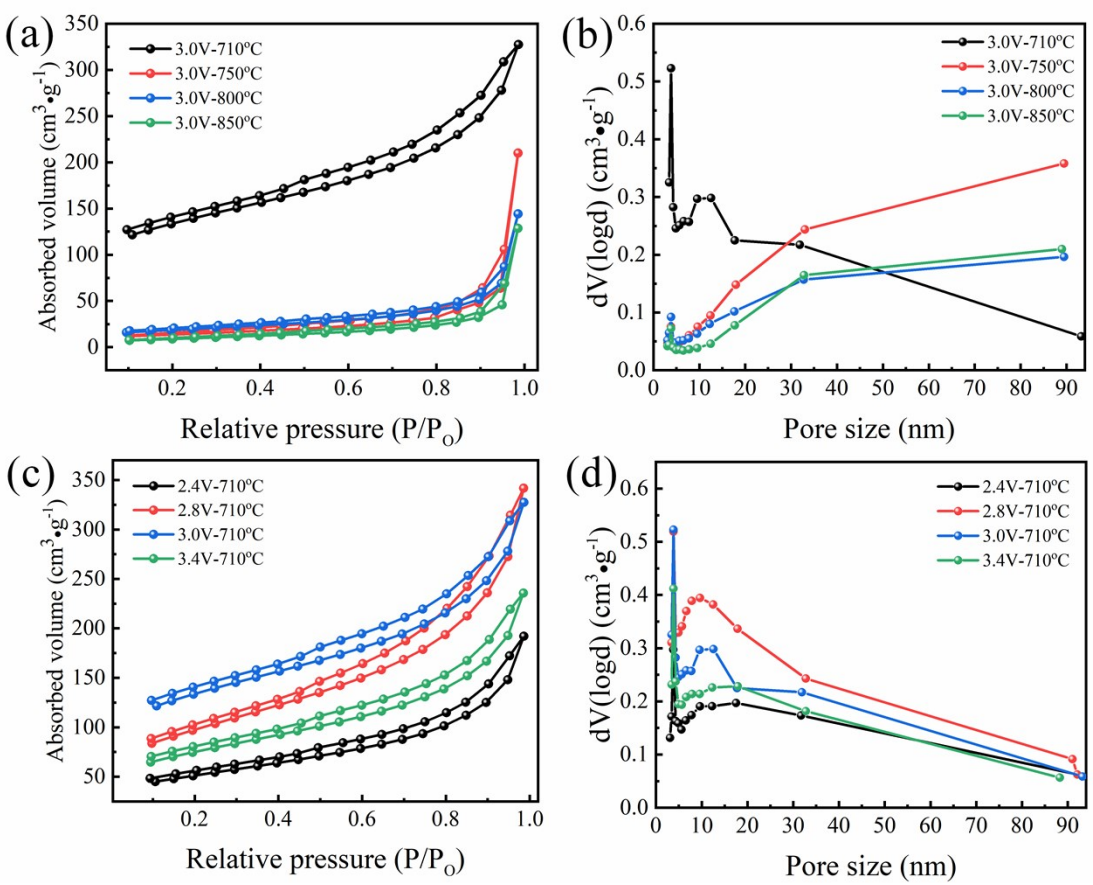

Fig. S6. (a, c) Nitrogen adsorption-desorption isotherms and (b, d) pore size distribution profiles of the electrolytic carbons obtained under indicated conditions.

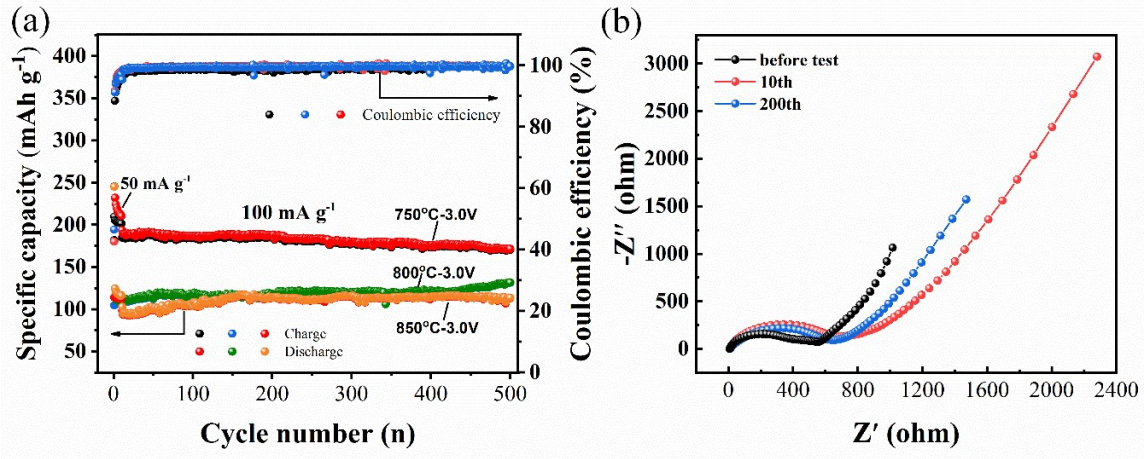

Fig. S7. Cycling performances of the electrolytic carbon obtained under different temperatures. (b) Nyquist plots of the EC-710-3.0 carbon at different cycles.

References

1. H. Ijije, R. Lawrence, G. Chen, *RSC Adv.*, 2014, **4**, 35808-35817.
2. W. Liu, J. Mei, G. Liu, Q. Kou, T. Yi, S. Xiao, *ACS Sustainable Chem. Eng.*, 2018, **6**, 11595-11605.
3. M. Ingram, B. Baron, G. Janz, *Electrochim. Acta.*, 1966, **11**, 1629-1639.
4. H. Kawamura, Y. Ito, *J. Appl. Electrochem.*, 2000, **30**, 571-574.
5. J. Ge, S. Wang, L. Hu, J. Zhu and S. Jiao, *Carbon.*, 2016, **98**, 649-657.
6. J. Ge, L. Hu, W. Wang, H. Jiao, S. Jiao, *ChemElectroChem.*, 2015, **2**, 224-230.
7. J. Ge, L. Hu, Y. Song, S. Jiao, *Faraday Discuss.*, 2016, **190**, 259-268.
8. B. Deng, J. Tang, X. Mao, Y. Song, H. Zhu, W. Xiao, D. Wang, *Environ. Sci. Technol.*, 2016, **50**, 10588-10595.
9. H. V. Ijije, C. Sun, G. Chen, *Carbon.*, 2014, **73**, 163-174.
10. H. Ijije, R. Lawrence, N. Siambun, S. Jeong, D. Jewell, D. Hu, G. Chen, *Faraday Discuss.*, 2014, **172**, 105-116.
11. H. Yin, X. Mao, D. Tang, W. Xiao, L. Xing, H. Zhu, D. Wang, D. R. Sadoway. *Energy Environ. Sci.*, 2013, **6**, 1538-1545.
12. S. Licht, B. Wang, S. Ghosh, H. Ayub, D. Jiang, J. Ganley, *J. Phys. Chem. Lett.*, 2010, **1**, 2363-2368.
13. L. Li, Z. Shi, B. Gao, J. Xu, X. Hu, Z. Wang, *J. Electrochem. Soc.*, 2016, **163**, E1-E2.
14. L. Li, Z. Shi, B. Gao, J. Xu, X. Hu, Z. Wang, *Electrochemistry.*, 2014, **82**, 1072-1077.
15. K. Le, H. Groult, F. Lantelme, M. Dubois, D. Avignant, A. Tressaud, S. Komaba, N. Kumagai, S. Sigrist, *Electrochim. Acta.*, 2009, **54**, 4566-4573.

16. D. Tang, H. Yin, X. Mao, W. Xiao, D. Wang, *Electrochim. Acta.*, 2013, **114**, 567-573.

17. B. Kaplan, H. Groult, A. Barhoun, F. Lantelme, T. Nakajima, V. Gupta, S. Komaba, N. Kumagai, *J. Electrochem. Soc.*, 2002, **149**, D72-D78.

18. D. Chery, V. Albin, V. Lair, M. Cassir, *Int. J. Hydrogen Energy.*, 2014, **39**, 12330-12339.

19. Y. Chen, Q. Xu, Q. Song, H. Li, Z. Ning, X. Lu, D. Fray, *Electrochem Commun.*, 2016, **64**, 1-4.

20. M. Hughes, J. Allen, S. Donne, *Electrochim. Acta.*, 2018, **278**, 340-351.